Article

Bacterial and Archaeal Assemblages from Two Size Fractions in Submarine Groundwater Near an Industrial Zone

Xiaogang Chen [iD], **Qi Ye ***, **Jinzhou Du** and **Jing Zhang**

State Key Laboratory of Estuarine and Coastal Research, East China Normal University, Shanghai 200062, China; xiaogangchen@outlook.com (X.C.); jzdu@sklec.ecnu.edu.cn (J.D.); jzhang@sklec.ecnu.edu.cn (J.Z.)

* Correspondence: qye@sklec.ecnu.edu.cn

check for updates

Abstract: Nutrients and organic pollutants transported by submarine groundwater discharge (SGD) play a significant role in controlling water quality, and can lead to the concerned deleterious effects on marine ecosystems. Subterranean estuaries are complicated habitats of diverse microbial communities that mediate different biogeochemical processes. However, there is less information on how microorganisms mediate biogeochemical cycles in the submarine groundwater system. In this study, we investigated the changes in bacterial and archaeal assemblages from two size fractions (0.2–0.45 μm and >0.45 μm) in the submarine groundwater of Qinzhou Bay, China. Phylogenetic analysis showed that *Bathyarchaeota* was dominant in archaeal communities in the >0.45 μm size fraction, but was seldom in the 0.2–0.45 μm fraction. The co-occurrence of sequences belonging to *Bathyarchaeota* and *Methanosaeta* was found in the >0.45 μm size fraction. Since a gene encoding acetate kinase of *Bathyarchaeota* is involved in acetate production, and acetate is also a necessary growth factor for *Methanosaeta*, the acetate produced by *Bathyarchaeota* can provide food or energy sources for *Methanosaeta* in this very >0.45 μm size fraction. The most abundant bacterial sequences in the >0.45 μm size fraction was closely related to biomineral iron-oxidizing *Gallionella* spp., whereas the dominant bacterial sequences in the 0.2–0.45 μm fraction were affiliated with *Limnohabitans* spp., which can utilize dissolved organic matter as an important source of growth substrates. Notably, approximately 10% of the bacterial sequences in both of the two size fractions belonged to *Novosphingobium* spp., which plays an important role in the degradation of pollutants, especially aromatic compounds. Furthermore, the predictive functional profiling also revealed that the pathways involved in the degradation of aromatic compounds by both bacteria and archaea were identified. The presence of nutrients or pollutants in our study site provides different substrates for the growth of the specific microbial groups; in turn, these microbes may help to deplete pollutants to the ocean through submarine groundwater. We suggest that these specific microbial groups could be potential candidates for effective in situ bioremediation of groundwater ecosystems.

Keywords: subterranean estuary; size fractions; bacteria, archaea; geochemistry; *Bathyarchaeota*; in situ bioremediation; Qinzhou Bay

1. Introduction

Submarine groundwater discharge (SGD) is defined as all the water flow on continental margins from the seabed to the coastal ocean, without regard to their fluid composition or driving force [1]. Compared with surface water, submarine groundwater has a different geochemistry, and where these waters mix prior to discharging, they form reactive zones known as the subterranean estuary [2]. The composition of SGD differs from that predicted by simple mixing, because biogeochemical reactions

in the aquifer modify its chemistry [3]. SGD fluxes of nutrients, metals, carbon and organic pollutants (e.g., pesticides, polychlorinated biphenyls (PCBs), polycyclic aromatic hydrocarbons (PAHs) and phthalates) are significant pathways from land to sea [3–5], and have been recognized to have negative effects, such as red tide outbreaks [6], eutrophication [7], and hypoxia [8], on marine ecological environments [9]. Therefore, SGD and its associated chemical substances are considered key parts of coastal management [10].

Qinzhou Bay is located in the south of Qinzhou City, Guangxi province, and is an industrial region greatly affected by industrial activities [11,12] (Figure 1). Recently, the natural ecosystem structure and marine ecological environment of this region have been changed because of industrialization and urbanization, such as the construction of large-scale petroleum refineries and pulp and paper mills [13,14]. Our recent work also revealed that significant SGD-derived nutrient and carbon fluxes exceeded river inputs in this region [11,12]. In this study, the sampling site is located in the Gaoshatou Village of Qinzhou Bay (Figure 1). The contamination of aromatic compounds often occurs near the industrial zone. For example, PCBs are widely used in industry, and their concentrations (ng g^{-1} dry wt) range from 1.62 to 62.6, with a mean of 9.87 in Qinzhou Bay [13]. The station with the highest PCBs concentration is very close to the compact district of the aforementioned petrochemical plants. However, there are no reports on the microbial compositions in the submarine groundwater of Qinzhou Bay, especially in different size fractions.
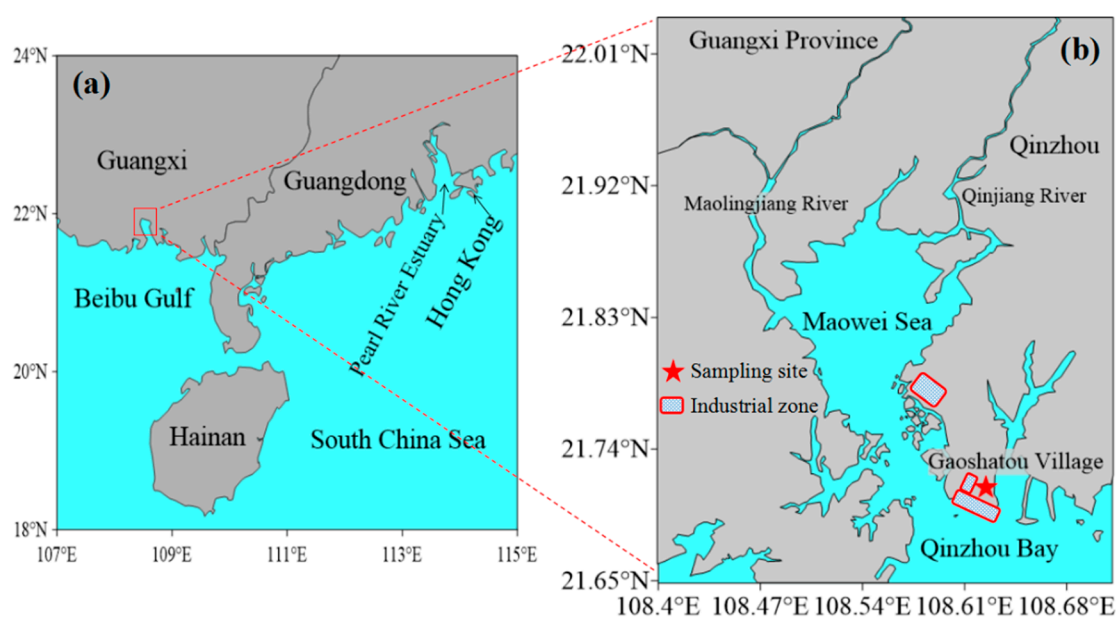

Figure 1. Map showing the study site location (**a**), sampling site and industrial zone (**b**) in Qinzhou Bay.

Suspended particulate matter (SPM) (>0.45 μm) is one of the main forms of nutrients, that is, carbon and organic pollutants which are transferred from land to the marine environment [15,16]. Composed of nutrients, organic micro-pollutants and heavy metals, SPM can affect material exchange and biogeochemical processes in coastal systems [15,17]. A number of studies demonstrated that microbial community composition, abundance and activity vary between the water and SPM in coastal surface water (e.g., [18–20]).

However, there are few reports on microorganisms from different size fractions in SGD, especially with reference to microorganisms attached to SPM. SGD is now globally recognized as one of the most important and central processes of land-ocean interaction in coastal zones [3]. Previous studies suggested that SGD is a significant pathway for fecal indicator bacteria to enter coastal waters in submarine groundwater contaminated by sewage, through activities such as waste treatment and disposal (e.g., [21]). In our previous work, bacterial diversity and distribution were investigated in

SGD along the coastal zone of the Yellow Sea, and we found some potential key bacterial groups, such as *Comamonas* spp., that may be excellent candidates for the bioremediation of natural pollutants in the SGD [22].

Microorganisms play an important role in mediating biochemical reactions within groundwater systems [21,23]. In this study, 16S rRNA gene-based MiSeq Illumina sequencing approach and PICRUSt (Phylogenetic Investigation of Communities by Reconstruction of Unobserved States) were used to analyze the bacterial and archaeal community compositions, and predict functional profiling between the 0.2–0.45 μm and >0.45 μm fractions (i.e., SPM) in the submarine groundwater of Qinzhou Bay, China, respectively. The objective of this work was (1) to explore the specific microbial groups in these two different size fractions, which could play an important ecological role in biogeochemical cycles in SGD to coastal zones. (2) To identify potential microbial candidates for in situ bioremediation/biodegradation in coastal groundwater ecosystems, and then provide valuable information for coastal environmental management.

2. Materials and Methods

2.1. Sample Collection and Measurements of Chemical Parameters

The samples were collected during March 2017, from an abandoned well near an industry zone in the Gaoshatou Village of Qinzhou Bay (Figure 1). Well water near the coasts is typical submarine groundwater, and can result in significant impacts on marine ecosystems [1,9,22]. In this study, submarine groundwater was collected by using an organic glass hydrophore [11,12]. The salinity and temperature were measured by a YSI-EC300A conductivity meter (YSI Inc., Yellow Springs, OH, USA) in the field. ^{222}Rn samples were collected in glass bottles using the overflow method [11,12], and were immediately analyzed using the RAD7 detector (Durridge Co. Inc., Billerica, MA, USA). Nutrients, dissolved inorganic carbon (DIC), and dissolved organic carbon (DOC) samples, were collected using polyethylene bottles filtered by 0.45 μm cellulose acetate filters, and stored in the dark to inhibit microbial growth [12,24]. The nutrient concentrations (NO_2^-, NO_3^-, NH_4^+, PO_4^{3-} and SiO_3^{2-}) were then analyzed using an autoanalyzer (Model: Skalar SAN^{plus} system, Skalar Analytical B.V., Breda, The Netherlands) [24]. The concentration of dissolved inorganic nitrogen (DIN) was determined as the sum of NO_2^-, NO_3^- and NH_4^+. The dissolved inorganic phosphorus (DIP) and dissolved inorganic silicon (DSi) represent the concentrations of PO_4^{3-} and SiO_3^{2-}, respectively. The DIC and DOC were analyzed using a TOC Analyzer (TOC-VCPH, Shimadzu Co. Ltd., Kyoto, Japan) [12].

To collect 0.2–0.45 μm and >0.45 μm size fractions, ten liter samples of submarine groundwater were first filtered through 0.45 μm pore size cellulose acetate filters, then filtered through 0.2 μm pore size polycarbonate filters (Nuclepore Track-Etched Membrane, Whatman Inc. Clifton, NJ, USA). Since the heterogenic geological matrix and high dynamics of aquifers can change the biogeochemical parameters of submarine groundwater [11,25], to eliminate accidental errors caused by heterogeneity and dynamics, quadruplicate submarine groundwater samples were collected size fractions. Both the 0.45 μm pore size cellulose acetate filters and 0.2 μm pore size polycarbonate filters were placed in sterile 1.5 mL microcentrifuge tubes, and immediately stored at −20 °C onsite, then samples were subsequently stored at −80 °C until further analysis. The blank filter treated with sterile water of the same volume as in the environmental sample was used as a negative control.

2.2. DNA Extraction, PCR Amplification and Illumina MiSeq Sequencing

Total environmental DNA was extracted from quadruplicate filters (four 0.45 μm filters and four 0.2 μm filters) using the MoBio PowerWater® DNA Isolation Kit (MOBIO Laboratories, Carlsbad, CA, USA) according to the manufacturer's instructions. Both the concentration and purity of the DNA were assessed by spectrophotometry (NanoDrop ND1000 spectrophotometer, Thermo Fisher Scientific, Wilmington, DE, USA). The extracted DNA was stored at −20 °C until further analysis. The results of the DNA purity and the concentration for each sample were showed in Table S1.

Minimum numbers of polymerase chain reaction (PCR) cycles were performed, and three independent PCR mixtures were pooled for each sample to decrease PCR bias. The bacterial 16S rRNA genes containing V4–V5 hypervariable regions were amplified using primers 515F (5′-GTGCCAGCMGCCGCGG-3′) and 907R (5′-CCGTCAATTCMTTTRAGTTT-3′) [26], and the following amplification conditions: 2 min at 95 °C; followed by 25 cycles of 95 °C for 30 s, 30 s at 55 °C, and 30 s at 72 °C; and an extension at 72 °C for 5 min. The archaeal 16S rRNA genes were amplified using primers 524F10extF (5′-TGYCAGCCGCCGCGGTAA-3′) and Arch958RmodR (5′-YCCGGCGTTGAVTCCAATT-3′) [27], using the following amplification conditions: 3 min at 95 °C; followed by 35 cycles of 30 s at 95 °C, 30 s at 55 °C, and 45 s at 72 °C; and a final extension at 72 °C for 10 min.

For Illumina MiSeq sequencing, PCR products were purified using the AxyPrep DNA Gel Extraction Kit (Axygen Biosciences, Union City, CA, USA) according to the manufacturer's protocol, and then quantified by QuantiFluorTM-ST (Promega, Madison, WI, USA). Reaction mixtures were pooled in equimolar ratios, and paired-end reads were generated on an Illumina MiSeq PE250 (Majorbio Bio-Pharm Technology Co., Ltd., Shanghai, China). Negative control did not produce a detectable PCR fragment for either bacterial or archaeal 16S rRNA gene amplification.

2.3. Sequence Data Processing, OTU Clustering, and Taxonomic Assignment

Raw Illumina FASTQ files were demultiplexed, quality filtered and analyzed using Quantitative Insights into Microbial Ecology (QIIME) (version 1.17) (An open-source software pipeline available at http://qiime.sourceforge.net/) [28] with criteria described previously [29]. Operational taxonomic units (OTUs, 97% similarity cutoff) were clustered using UPARSE (version 7.1) (An open-source software pipeline available at http://drive5.com/uparse/). Chimeric sequences were screened using UCHIME. The abundances of OTUs from each sample was determined by OTU cluster. The number of reads from each sample was assigned to each out, and an "OTU table" was generated using the usearch_global command. To obtain the taxonomic information of each OTU corresponding species, the Ribosomal Database Project (RDP) Classifier (http://rdp.cme.msu.edu/) was used for taxonomic analysis of representative OTU sequences. The community composition of each sample was calculated at the genus level. Sequence data were entered into the NCBI Sequence Read Archive under BioProject ID PRJNA515097 (bacteria) and PRJNA515099 (archaea).

2.4. Phylogenetic Analyses

The sequences of the representative OTUs in this study were analyzed in GenBank by BLAST (https://blast.ncbi.nlm.nih.gov/Blast.cgi) to obtain reference sequences. The sequences of representative OTUs and selected reference sequences from the database were aligned using Clustal W. Then the phylogenetic trees were generated in MEGA6 using the neighbor-joining method with a bootstrap test of 1000 replicates and a maximum composite likelihood model [30].

2.5. Statistical Analyses

Alpha diversity metrics and coverage were calculated by the Mothur program [31]. As a visualization technique, principal-coordinate analyses (PCoA) using Bray-Curtis distance was performed to show if distinct separations in bacterial or archaeal community structures were present between the 0.2–0.45 μm and >0.45 μm size fractions. PERmutational Multivariate ANalysis Of VAriance (PERMANOVA) based on this Bray-Curtis distance was constructed in R package vegan. PERMANOVA calculation was performed using raw relative abundance data.

2.6. Predictive Functional Profiling

Based on the 16S rRNA gene sequences, PICRUSt was used to the predictive functional profiling of microbial communities [32]. First, the abundance of each OTU was normalized by the 16S rRNA gene copy number predictions. The abundance of Kyoto Encyclopedia of Genes and Genomes (KEGG)

Orthology was then calculated according to the greengenes ID of each OTU. Here, the greengenes ID is obtained from the Greengenes database (http://greengenes.lbl.gov/). The final output table of gene family counts was summarized as pathway-level categories.

3. Results

3.1. Site Description and Environmental Characteristics

The descriptions of the sampling site and environmental chemical parameters of submarine groundwater in this study are summarized in Table 1. The study site is close to the industrial zone of Qinzhou City, China. The temperature and salinity of the submarine groundwater were 17.2 °C and 0.5, respectively. The activity of ^{222}Rn in the studied well water (4140 Bq m^{-3}) was much higher than that of ^{222}Rn in the seawater (127 Bq m^{-3}) of Qinzhou Bay. Choosing a representative submarine groundwater end-member is always a key and difficult problem in SGD studies [11,12,25,33]. This is because representative submarine groundwater end-member must take into account the salinity, ^{222}Rn (an excellent SGD tracer) and the distance from the coastal line [11,12,25]. The values of salinity and ^{222}Rn in this studied well, as well as its position, indicated that the studied well water is a representative submarine groundwater end member. The DIC concentration of the submarine groundwater was 1.3 mmol L^{-1} and the DOC concentration was 1.0 mmol L^{-1}. The concentrations (μmol L^{-1}) of DIN, DIP and DSi in the studied submarine groundwater were 10.4, 0.31 and 166, respectively.

Table 1. Descriptions of the sampling site and environmental chemical parameters of submarine groundwater.

Site Descriptions		Environmental Chemical Parameters	
Latitude	21°43′39.92″ N	Temperature (°C)	17.2
Longitude	108°37′30.43″ E	Salinity	0.5
Location	Qinzhou City, Guangxi Province	^{222}Rn (Bq m^{-3})	4140
Well depth (m)	~ 4	DIC (mmol L^{-1})	1.3
Characteristics of sampling site	In the Gaoshatou Village; near an industrial zone; 800 meters from the coast; garbage found	DOC (mmol L^{-1}) NO$_3^-$ (μmol L^{-1}) NO$_2^-$ (μmol L^{-1})	1.0 5.2 0.42
Characteristics of submarine groundwater	Turbid water; smelly water	NH$_4^+$ (μmol L^{-1}) PO$_4^{3-}$ (μmol L^{-1}) SiO$_3^{2-}$ (μmol L^{-1})	4.8 0.31 166

3.2. Bacterial and Archaeal Diversity

To obtain insights into the microbial diversity of the submarine groundwater in Qinzhou Bay, we obtained a total of 240,429 high-quality bacterial V4-V5 Illumina sequences and 345,993 high-quality archaeal V4-V5 Illumina sequences in two size fractions. There were 22,776 bacterial reads and 24,760 archaeal reads per sample after subsampling (all samples were randomly resampled down to the smallest sample size). According to the 97% similarity cutoff, there were 1113 bacterial OTUs and 619 archaeal OTUs in the complete OTU data set. Among these OTUs, 756 common bacterial OTUs and 451 common archaeal OTUs were found in the two size fractions. Good's coverage was 99.1–99.9% for all samples. PCoA analysis showed that the bacterial community in the 0.2–0.45 μm fraction was clearly separated from that in the >0.45 μm fraction along the first axis, explaining 49.81% of the variation. Similarly, the archaeal community in the 0.2–0.45 μm fraction was clearly separated from that in the >0.45 μm fraction along the first axis explaining 85.69% of variation (Figure 2).

PCoA analysis also showed that the spatial pattern of the bacterial community in the two size fractions was opposite to the archaeal community, which may indicate that the spatial niche partitioning

of bacterial and archaeal communities was different in the two size fractions of submarine groundwater. However, we found that quadruplicate submarine groundwater samples of bacteria and archaea in the 0.2–0.45 μm fraction were also separated, which may be attributed to the heterogenic geological matrix and high dynamics of aquifers [11,25]. In addition, the R^2 and *p* values were calculated using the PERMANOVA approach, which showed that significant differences were found in both bacteria (PERMANOVA, n = 4, R^2 = 0.51, *p* < 0.05) and archaea (PERMANOVA, n = 4, R^2 = 0.78, *p* < 0.05) between the >0.45 μm size fraction and the 0.2–0.45 μm fraction (Table 2).

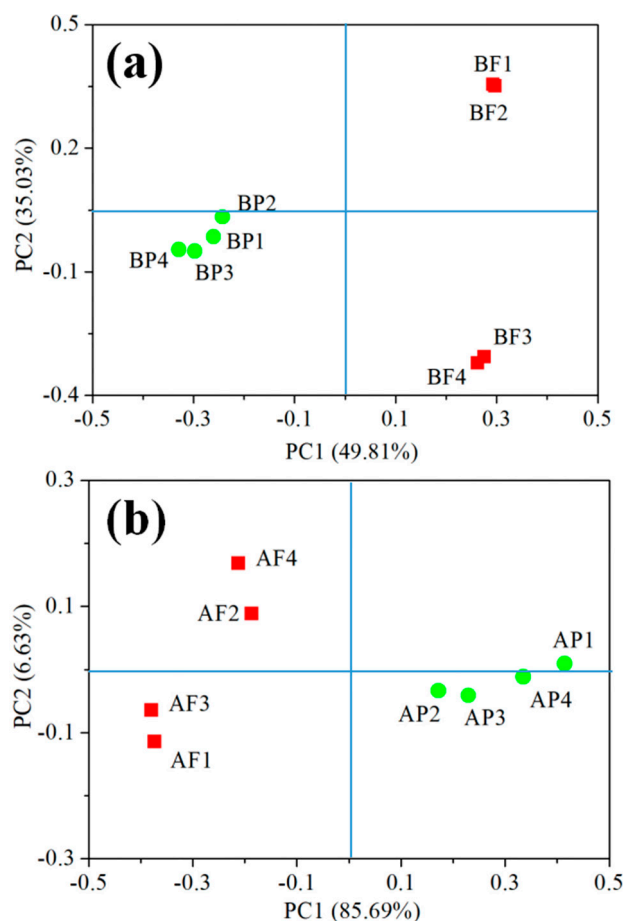**Figure 2.** The principal-coordinate analyses (PCoA) analysis on operational taxonomic unit (OTU) levels of main bacterial (**a**) and archaeal (**b**) genera from >0.45 μm (green dots) and 0.2–0.45 μm (red squares) size fractions. BP and BF represent bacteria of >0.45 μm and 0.2–0.45 μm size fractions, respectively. AP and AF represent archaea of >0.45 μm and 0.2–0.45 μm size fractions, respectively. The values of 1–4 represent four parallel samples.

Table 2. Calculations of Statistic R^2 and *p* values using the PERmutational Multivariate ANalysis of VAriance (PERMANOVA) approach.

Method	Distance	Bacteria		Archaea	
		R^2	*p* Value	R^2	*p* Value
PERMANOVA	Bray-Curtis	0.51	0.02	0.78	0.02

3.3. Bacterial and Archaeal Distribution

Taxonomic distributions show that there were some differences in the proportion of Illumina sequences between the >0.45 μm size fraction and the 0.2–0.45 μm fraction, respectively (Figure 3). Each percentile value in the parenthesis in the text below is the mean value of quadruplicate analyses.

Limnohabitans and *Gallionella* were the most abundant genera in the 0.2–0.45 μm fraction (26.6%) and the >0.45 μm size fraction (16.7%) in bacterial samples, respectively. However, *Limnohabitans* existed in both size fractions, but *Gallionella* only existed in the >0.45 μm size fraction. The reason may be that *Gallionella* need to obtain energy for growth from Fe(II) oxidation and facilitate the precipitation of Fe(III) oxyhydroxides [34]. The second dominant groups were *Candidatus Planktophila* in the 0.2–0.45 μm fraction (8.8%) and *Novosphingobium* in the >0.45 μm size fraction (11.5%) in bacterial samples. *Bathyarchaeota* (32.5%) was the most abundant genus in the >0.45 μm size fraction archaeal sample and *Methanosaeta* (19.9%) formed the second dominant group in the >0.45 μm size fraction archaeal sample. However, *Bathyarchaeota* (3.3%) was seldom detected in the 0.2–0.45 μm size fraction. In addition, a large number of archaeal sequences (i.e., others: 51.1%) were remotely related to the reported environmental sequences in the database in the 0.2–0.45 μm size fraction, showing the archaeal communities in the 0.2–0.45 μm size fraction had more diversity.
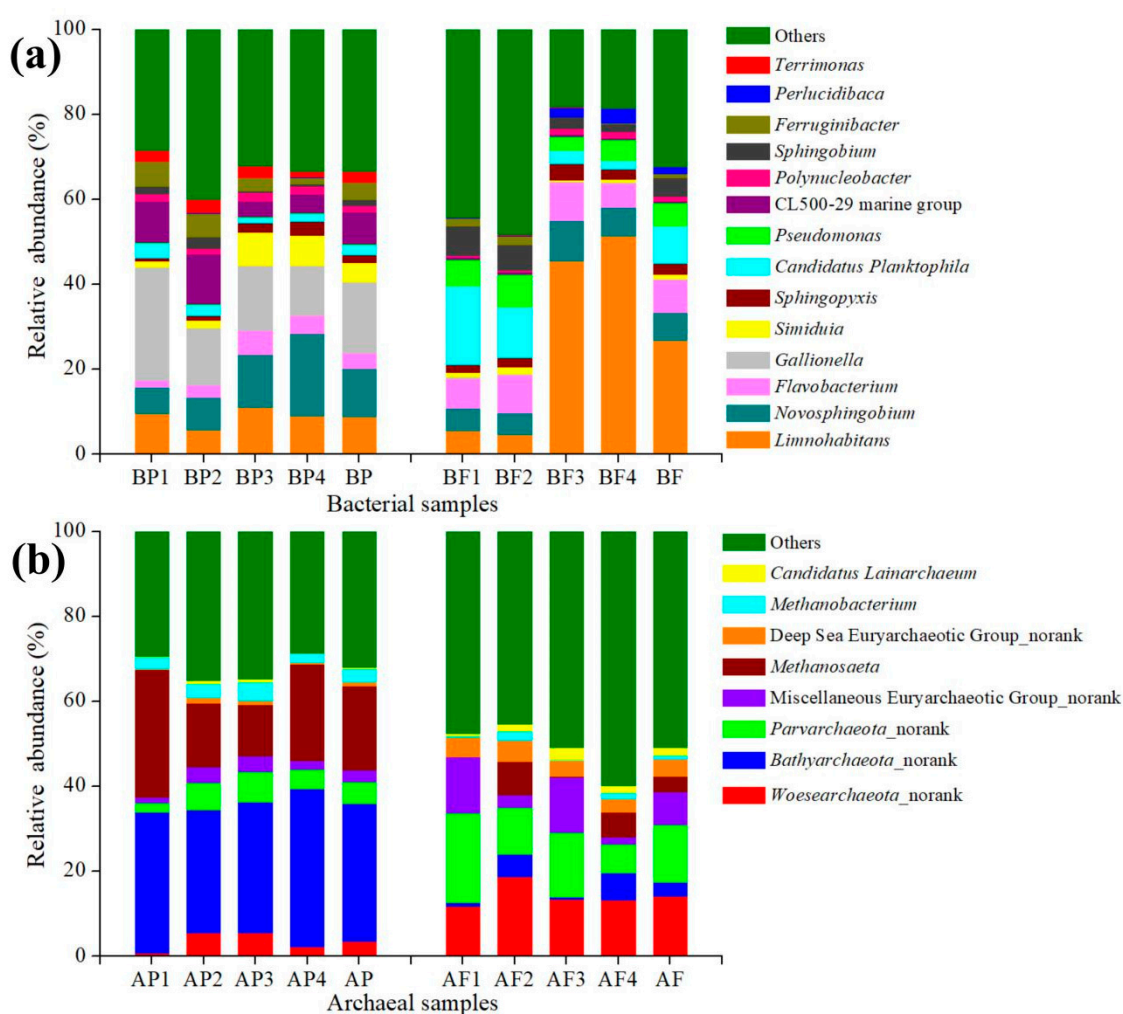

Figure 3. Distributions of genus-level taxa for bacterial (**a**) and archaeal (**b**) samples. Bars represent the proportion of sequences represented by each genus. Bacterial taxa represented by less than 2% reads are pooled as "others". The designation "norank" means that the specific archaeal taxa cannot be classified at the genus level. The proportion of each sequence in two size fractions is the mean value of quadruplicate analyses. BP, BF, AP and AF represent the average values of BP1–BP4, BF1–BF4, AP1–AP4 and AF1–AF4, respectively.

3.4. Phylogenetic Analyses

3.4.1. Main Bacterial Groups in Two Size Fractions

A bacterial analysis detected OTUs related to *Betaproteobacteria*, *Gammaproteobacteria*, *Alphaproteobacteria*, *Actinobacteria*, *Flavobacteria* and *Sphingobacteria* within the >0.45 μm size fraction and the 0.2–0.45 μm fraction (Figure 4). As shown in Table 3, the betaproteobacterial sequences of OTU 594 were the most abundant genus in the 0.2–0.45 μm fraction (21.8%), and were also found in the >0.45 μm size fraction (4.7%) and exhibited 99.2% similarity with the *Limnohabitans australis* strain MWH-BRAZ-DAM2D (NR_125544) [35]. Sequences of OTU 571 were obtained from the >0.45 μm size fraction (1.2%) and the 0.2–0.45 μm fraction (2.6%), and showed 98.9% similarity with the *Limnohabitans parvus* strain II-B4 (NR_125542) [36]. The betaproteobacterial sequences of OTU 40 were the most abundant genus in the >0.45 μm size fraction (16.6%), but were few in the 0.2–0.45 μm fraction (0.2%); this OTU had 98.9% similarity with the clone F22F60 from a Fe(II)-oxidizing, nitrate-reducing enrichment culture (FN430660) [37]. OTU 1039 was found in the >0.45 μm size fraction (4.5%), but there were very few in the 0.2–0.45 μm fraction (0.8%); this OTU was phylogenetically associated (99.7% similarity) with the gammaproteobacterial clone SWL18 from a sludge wastewater treatment system (AY528817) [38]. The alphaproteobacterial sequences of OTU 261 and OTU 555 were found in the >0.45 μm size fraction (10.7% for OTU 261 and 1.2% for OTU 555) and the 0.2–0.45 μm fraction (5.4% for OTU 261 and 1.5% for OTU 555). OTU 261 had 98.4% similarity with the *Novosphingobium pentaromativorans* strain US6-1 (NR_025248), which is an aromatic hydrocarbon-degrading bacterium isolated from estuarine sediment [39], and OTU 555 had 99.2% similarity with the *Sphingopyxis soli* strain BL03 (NR_116739) [40]. Two OTUs displayed relatively high identities with representatives within the class *Flavobacteria*. OTU 843, representing 3.1% and 2.7% of the >0.45 μm size fraction and 0.2–0.45 μm fraction, respectively, had 98.7% similarity with the *Flavobacterium chungnamense* strain ARSA-103 (NR_117494) [41]. OTU 591 comprised 0.1% and 1.6% sequences in the >0.45 μm size fraction and the 0.2–0.45 μm fraction, respectively, and had 98.4% similarity with the *Flavobacterium columnare* strain ATCC 23463 (NR_118582) [42].

Table 3. Closest relatives of main OTUs in bacterial samples.

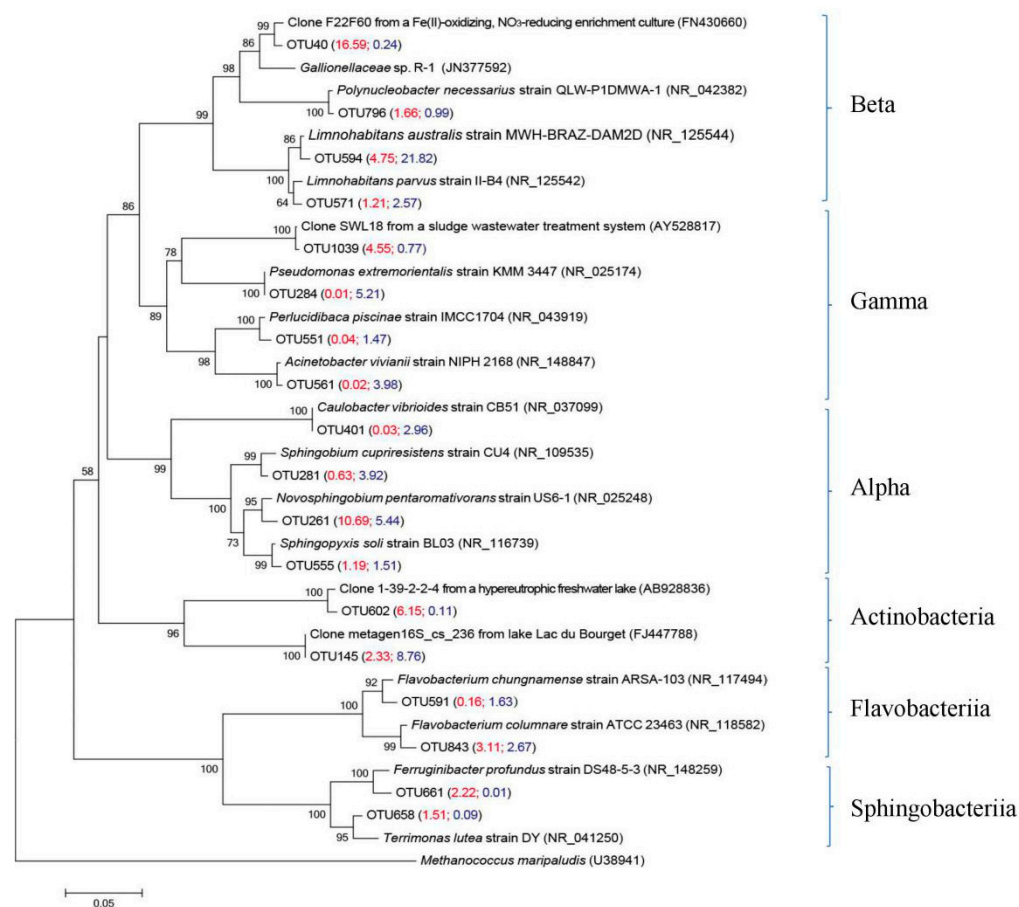| OTU	Proportion of OTUs (%)		Closest Relatives	Similarity
	BP	BF		
OTU 594	4.7	21.8	*Limnohabitans australis* strain MWH-BRAZ-DAM2D [35]	NR_125544 (99.2%)
OTU 571	1.2	2.6	*Limnohabitans parvus* strain II-B4 [36]	NR_125542 (98.9%)
OTU 40	16.6	0.2	Clone F22F60 from a Fe(II)-oxidizing, nitrate-reducing enrichment culture [37]	FN430660 (98.9%)
OTU 1039	4.5	0.8	Gammaproteobacterial clone SWL18 from a sludge wastewater treatment system [38]	AY528817 (99.7%)
OTU 261	10.7	5.4	*Novosphingobium pentaromativorans* strain US6-1 [39]	NR_025248 (98.4%)
OTU 555	1.2	1.5	*Sphingopyxis soli* strain BL03 [40]	NR_116739 (99.2%)
OTU 843	3.1	2.7	*Flavobacterium chungnamense* strain ARSA-103 [41]	NR_117494 (98.7%)
OTU 591	0.1	1.6	*Flavobacterium columnare* strain ATCC 23463 [42]	NR_118582 (98.4%)

Figure 4. Neighbor-joining phylogenetic tree based on 16S rRNA gene sequences showing the phylogenetic relationship among the representative bacterial OTUs obtained in the >0.45 μm size fraction and the 0.2–0.45 μm fraction and reference 16S rRNA gene sequences retrieved from the NCBI GenBank. These bacterial OTUs were represented by the top 10 reads from the >0.45 μm size fraction and the 0.2–0.45 μm fraction. The scale bar represents the estimated number of nucleotide changes per sequence position. Percentage numbers on nodes refer to 1000 bootstrap resamplings conducted. Only values >50% are shown. Bold bacterial OTUs were obtained from the >0.45 μm size fraction and the 0.2–0.45 μm fraction. The numbers in parentheses indicate the percentage composition of reads in each sample in the following order: (BP, BF). *Methanococcus maripaludis* (U38941) was used as the outgroup. The number in parentheses represents the mean value of quadruplicate analyses.

3.4.2. Main Archaeal Groups in Two Size Fractions

In the archaeal analysis, OTUs related to *Bathyarchaeota*, *Euryarchaeota*, *Parvarchaeota*, and *Woesearchaeota* were detected within the >0.45 μm size fraction and the 0.2–0.45 μm fraction (Figure 5). As shown in Table 4, phylogenetic analysis showed that three representative OTUs (OTU 563, 516 and 598) belonging to the phylum *Bathyarchaeota* were dominant in archaeal communities in the >0.45 μm size fraction (29.4%), but were seldom detected in the 0.2–0.45 μm fraction (3.0%). OTU 563 exhibited 100% similarity with clone R5ENDA4 from low-temperature anaerobic solvent-degrading bioreactors (DQ399807) [43]. OTU 516 showed 100% similarity with clone ASC27 in unsaturated, petroleum-contaminated soil (AB161330) [44], and OTU 598 had 100% similarity with clone ASC37 in unsaturated, petroleum-contaminated soil (AB161337) [44]. Euryarchaeotal OTU 540 was found in the >0.45 μm size fraction (19.5%), but was seldom detected in the 0.2–0.45 μm fraction (3.3%); this OTU gave a 99.6% match to the acetoclastic methanoarchaeon *Methanosaeta concilii* strain GP6 (NR_102903) [45]. Within the Miscellaneous Euryarchaeotic Group (MEG), OTU 312 was found in the >0.45 μm size fraction (1.1%) and 0.2–0.45 μm fraction (3.7%) and had 99.2% similarity with

DGGE (Denaturing Gradient Gel Electrophoresis) gel band VIARC-174 from the water column of Lake Vilar (EU683427) [46]. Phylum *Parvarchaeota* was found in the >0.45 μm size fraction (3.2%) and the 0.2–0.45 μm fraction (7.4%). Representative OTU 458 had 98.4% similarity with the clone WsL03b13_109f from groundwater of a volcanic mountain, Mt. Fuji (AB794582) (Unpublished). The sequences related to phylum *Woesearchaeota* including OTU 536 and OTU 541 were found in the >0.45 μm size fraction (1.8% for OTU 536 and 0.5% for OTU 541) and the 0.2–0.45 μm fraction (5.7% for OTU 536 and 2.3% for OTU 541). OTU 536 had 98.8% similarity with clone LL_ADT_15 from low-level bank soil of the River Rhine (AM503273) [47], and OTU 541 had only 87.0% similarity with clone gwa2_scaffold_29719 from an aquifer adjacent to Colorado River (KP308734) [48]. Another important finding in this study is that the unidentified sequences of OTU 449 were abundantly found in the >0.45 μm size fraction (16.3%) and the 0.2–0.45 μm fraction (41.4%). This OTU had 92.5% similarity with VIARC-45 (AM697998) retrieved from the water column of Lake Vilar. VIARC-45 was grouped within Deep-Sea Hydrothermal Vent Euryarchaeotal Group 6 (DHVG-6) [46].
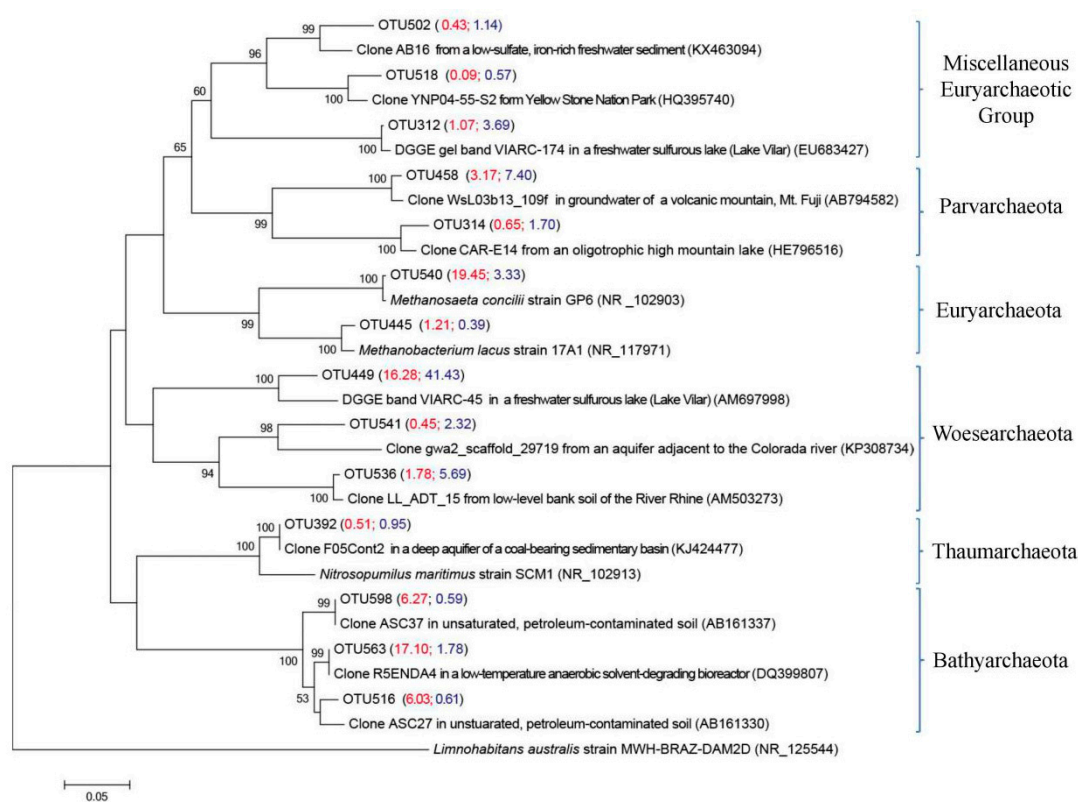

Figure 5. Neighbor-joining phylogenetic tree based on 16S rRNA gene sequences showing the phylogenetic relationship among the representative archaeal OTUs obtained in the >0.45 μm size fraction and the 0.2–0.45 μm fraction and reference 16S rRNA gene sequences retrieved from the NCBI GenBank. These archaeal OTUs were represented by the top 10 reads from the >0.45 μm size fraction and the 0.2–0.45 μm fraction. The scale bar represents the estimated number of nucleotide changes per sequence position. Percentage numbers on nodes refer to 1000 bootstrap resamplings conducted. Only values >50% are shown. Bold archaeal OTUs were obtained from the >0.45 μm size fraction and the 0.2–0.45 μm fraction. The numbers in parentheses indicate the percentage composition of reads in each sample in the following order: (AP, AF). *Limnohabitans australis* strain MWH-BRAZ-DAM2D (NR_125544) was used as the outgroup. The number in parentheses represents the mean value of quadruplicate analyses.

Table 4. Closest relatives of main OTUs in archaeal samples.

| OTU | Proportion of OTUs (%) | | Closest Relatives | Similarity |
	AP	AF		
OTU 563			Clone R5ENDA4 from low-temperature anaerobic solvent-degrading bioreactors [43]	DQ399807 (100%)
OTU 516	29.4 (OTU 563, 516 and 598)	3.0 (OTU 563, 516 and 598)	Clone ASC27 in unsaturated, petroleum-contaminated soil [44]	AB161330 (100%)
OTU 598			Clone ASC37 in unsaturated, petroleum-contaminated soil [44]	AB161337 (100%)
OTU 540	19.5	3.3	Acetoclastic methanoarchaeon *Methanosaeta concilii* strain GP6 [45]	NR_102903 (99.6%)
OTU 312	1.1	3.7	DGGE gel band VIARC-174 from the water column of Lake Vilar [46]	EU683427 (99.2%)
OTU 458	3.2	7.4	Clone WsL03b13_109f from groundwater of a volcanic mountain, Mt. Fuji (Unpublished)	AB794582 (98.4%)
OTU 536	1.8	5.7	Clone LL_ADT_15 from low-level bank soil of the River Rhine [47]	AM503273 (98.8%)
OTU 541	0.5	2.3	Clone gwa2_scaffold_29719 from an aquifer adjacent to Colorado River [48]	KP308734 (87.0%)
OTU 449	16.3	41.4	VIARC-45 retrieved from the water column of Lake Vilar [46]	AM697998 (92.5%)

3.5. Distinct Bacterial and Archaeal Communities in Two Size Fractions

In this study, *Gallionella* spp. and *Limnohabitans* spp. constituted the major group in the >0.45 μm size fraction and the 0.2–0.45 μm fraction, respectively. Meanwhile, phylogenetic analysis showed that the dominant archaeal phylum in the >0.45 μm size fraction was *Bathyarchaeota*, which was seldom detected in the 0.2–0.45 μm size fraction. In most cases, 0.45 μm pore size membrane filters are commonly used to collect SPM samples [17], especially for geochemists. Therefore, to analyze the bacterial and archaeal communities attached to SPM, we used 0.45 μm pore size cellulose acetate membranes to collect the samples in the >0.45 μm size fraction. We found that *Bathyarchaeota* was dominant in archaeal communities in the >0.45 μm size fraction, but was seldom detected in the 0.2–0.45 μm size fraction, indicating that *Bathyarchaeota* were preferentially attached to the SPM with a particle size greater than 0.45 μm.

4. Discussion

4.1. The Ecological Niches of Bathyarchaeota in Submarine Groundwater Systems

Phylogenetic analysis showed that the dominant archaeal group in the >0.45 μm size fraction was *Bathyarchaeota*. This *Bathyarchaeota*, which was formerly known as the Miscellaneous Crenarchaeotal Group (MCG), dominates marine subsurface archaeal communities [49,50] and has not yet been successfully cultured in the laboratory due to the slow growth rate of these microbes [51]. Recently, four genomic bins (MCG-6, MCG-1, MCG-7/17 and MCG-15) were found to belong to different *Bathyarchaeota* subgroups 6, 1, 7/17 and 15 [52]. *Bathyarchaeota* subgroup 6 has been proposed to have the ability to hydrolyze extracellular plant-derived carbohydrates, and degrade detritus proteins by metabolic predictions [52]. Meanwhile, all four subgroups have been shown to possess genes encoding enzymes involved in acetate production and the reductive acetyl-CoA pathway, suggesting that four subgroups of *Bathyarchaeota* are organo-heterotrophic and autotrophic acetogens, and these subgroups also have a potential metabolic pathway for dissimilatory nitrite reduction to ammonium [52]. In this study, we found that three dominant bathyarchaeotal OTUs (OTU 563, 516 and 598) were affiliated with our *Bathyarchaeota* subgroup 6 (Figure 6), showing similar ecological potentials to those of this subgroup 6. Based upon the estimation of chemical rates, *Bathyarchaeota* have been identified as some of the most

active microbial groups in the deep marine biosphere [53]. Some studies have found that *Bathyarchaeota* not only has metabolic pathways to degrade complex organic compounds such as aromatic compounds, cellulose, chitin and proteins, but also can use hydrogen and CO_2 to produce acetate [50,52,54,55]. Metabolic reconstruction based on genomic bins assembled from the metagenome found that the acetate produced by acetogenic *Bathyarchaeota* is an important electron carrier, and may be consumed by heterotrophic bacteria and acetoclastic methanogens, where the acetogenic *Bathyarchaeota* are key players in carbon cycling and ecosystems in marine sediments [55]. However, to our knowledge, there are few reports on the *Bathyarchaeota* in the submarine groundwater systems. Our results suggest that *Bathyarchaeota* are not only active and key players in carbon cycling and ecosystems in the deep marine biosphere, but also significant participants in carbon metabolism in submarine groundwater systems.
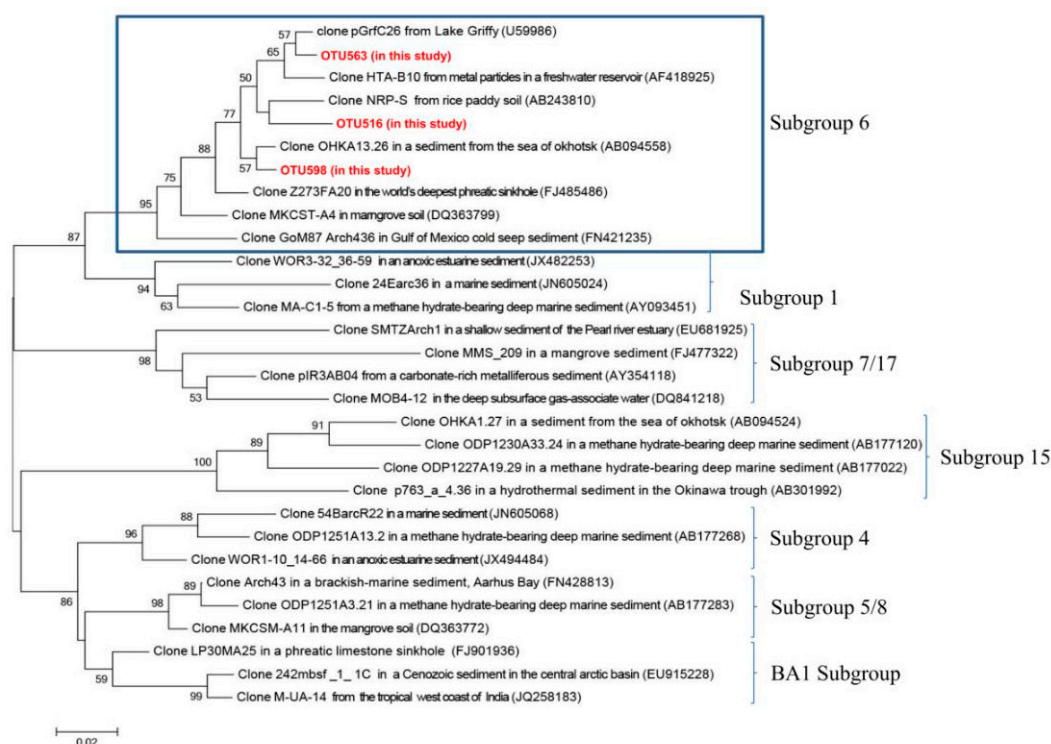

Figure 6. Neighbor-joining phylogenetic tree showing the placement of three representative bathyarchaeotal OTUs in the study in the *Bathyarchaeota* subgroup 6. The reference sequences of different *Bathyarchaeota* subgroups are according to [52]. The scale bar represents the estimated number of nucleotide changes per sequence position. Percentage numbers on nodes refer to 1000 bootstrap resamplings conducted. Only values >50% are shown.

In addition, the BA1 and BA2 genomes of *Bathyarchaeota* contain divergent homologs of the genes necessary for methane metabolism obtained from metagenomic analysis [51]. *Bathyarchaeota* may play an important ecological role via a potential symbiotic association with *Methanosaeta* [56]. Acetate is an important organic substrate for the growth and methane production of acetoclastic *Methanosaeta* [57]. Meanwhile, a gene encoding acetate kinase of *Bathyarchaeota* could also be involved in acetate production [55,56]. In this study, the co-occurrence of sequences belonging to *Bathyarchaeota* and the genus *Methanosaeta* was found in the >0.45 μm size fraction, indicating possible acetate production by members of *Bathyarchaeota* in SPM. Since the concentrations of organic compounds such as PAHs in SPM were very high in comparison with those in water in a coastal ecosystem [58], SPM could provide a source of nutrients for *Bathyarchaeota*. The metabolic produced by *Bathyarchaeota*, such as acetate, can also serve as food or energy sources for *Methanosaeta*. Therefore, we speculate that these two groups prefer living in the >0.45 μm size fraction. Meanwhile, these processes of *Bathyarchaeota*

and *Methanosaeta* not only could indicate the existence of a syntrophic association between these two groups, but also may explain the mechanism of symbiosis between *Bathyarchaeota* and *Methanosaeta* [56].

4.2. Microbial Candidate for In Situ Bioremediation in SGD

The in situ biodegradation or bioremediation of groundwater contamination has gradually gained more attention because it is more cost effective than commercial inoculum [59]. In this study, approximately 10% of bacterial sequences in both the >0.45 μm size fraction and the 0.2–0.45 μm fraction belonged to *Novosphingobium* spp. This *Novosphingobium* is a genus within the alpha subclass of *Proteobacteria* [60]; this subclass includes species of the genus *Sphingomonas* [61]. This bacterial group plays an important role in the degradation of aromatic compounds, such as PAHs, carbofuran, pentachlorophenol (PCP), and estrogen [60,62–65].

The dominant archaeal communities in the >0.45 μm size fraction in this study were *Bathyarchaeota*, which can also degrade aromatic compounds into small-molecule compounds, such as acetate [55]. Acetate is an important electron carrier, and may be consumed by heterotrophic bacteria and acetoclastic methanogens [55]. To further prove the accuracy of our results, the PICRUSt approach [32] was proposed to predict the abundance of functional categories (KEGG metabolic pathways) using 16S rRNA gene sequences in our study. The pathways involved in the degradation of aromatic compounds by both bacteria and archaea were identified and are shown in Tables 5 and 6. Therefore, the high abundance of *Bathyarchaeota* in the >0.45 μm size fraction and *Novosphingobium* spp. in the >0.45 μm size fraction and the 0.2–0.45 μm fraction in our samples indicated that these species could be selected as microbial candidates for in situ biodegradation or bioremediation in polluted submarine groundwater.

As a significant component of iron cycling [66], Fe(II)-oxidizing bacteria (FeOB) of the family *Gallionellaceae* can obtain energy for growth by catalyzing the oxidation of Fe(II) [67] and then form Fe(III) mineral precipitation [34]. The sequences of OTU 40 showed 98.9% similarity with clone F22F60 from a Fe(II)-oxidizing, nitrate-reducing enrichment culture (FN430660) [37]. This process could cause Fe(II) oxidation and form Fe(III) mineral precipitation while consuming nitrate and producing N_2 [37]. Because this process can reduce the concentration of nitrate in SGD, it plays a very important role in alleviating environmental problems caused by high concentrations of SGD-derived nitrate. The most abundant bacterial OTU, OTU 594, in the 0.2–0.45 μm fraction, was affiliated with *Limnohabitans* spp., which are characterized by high growth rates, metabolic flexibility and a preference for phytoplankton-derived organic material [68,69]. In addition, photolysis products of dissolved organic matter (DOM) have been suggested as an important source of substrates for *Limnohabitans* spp. [70–72]. Therefore, *Gallionella* spp. and *Limnohabitans* spp. in SGD could also be selected as microbial candidates for in situ biodegradation/bioremediation.

Table 5. Kyoto Encyclopedia of Genes and Genomes (KEGG) metabolic pathways involved in the degradation of aromatic compounds in bacterial samples.

Pathway	Relative Abundance		Definition
	>0.45 μm Size Fraction	0.2–0.45 μm Fraction	
ko00351	0.00	0.00	1,1,1-Trichloro-2,2-bis(4-chlorophenyl)ethane (DDT) degradation
ko00361	0.22	0.21	Chlorocyclohexane and chlorobenzene degradation
ko00362	1.31	1.55	Benzoate degradation
ko00363	0.19	0.23	Bisphenol degradation
ko00364	0.13	0.12	Fluorobenzoate degradation
ko00621	0.21	0.18	Dioxin degradation
ko00622	0.20	0.15	Xylene degradation
ko00623	0.34	0.34	Toluene degradation
ko00624	0.27	0.29	Polycyclic aromatic hydrocarbon degradation
ko00625	0.50	0.52	Chloroalkane and chloroalkene degradation
ko00626	0.48	0.54	Naphthalene degradation
ko00627	0.88	1.09	Aminobenzoate degradation
ko00633	0.16	0.13	Nitrotoluene degradation
ko00642	0.22	0.18	Ethylbenzene degradation
ko00643	0.20	0.20	Styrene degradation
ko00791	0.10	0.10	Atrazine degradation
ko00903	0.76	0.92	Limonene and pinene degradation
ko00930	0.56	0.70	Caprolactam degradation
Total	6.73	7.46	

Table 6. KEGG metabolic pathways involved in the degradation of aromatic compounds in archaeal samples.

Pathway	Relative Abundance		Definition
	>0.45 μm Size Fraction	0.2–0.45 μm Fraction	
ko00281	0.19	0.25	Geraniol degradation
ko00361	0.01	0.03	Chlorocyclohexane and chlorobenzene degradation
ko00362	0.49	0.53	Benzoate degradation
ko00363	0.01	0.04	Bisphenol degradation
ko00364	0.00	0.01	Fluorobenzoate degradation
ko00621	0.01	0.03	Dioxin degradation
ko00622	0.00	0.01	Xylene degradation
ko00623	0.33	0.29	Toluene degradation
ko00624	0.11	0.12	Polycyclic aromatic hydrocarbon degradation
ko00625	0.17	0.23	Chloroalkane and chloroalkene degradation
ko00626	0.05	0.11	Naphthalene degradation
ko00627	0.23	0.29	Aminobenzoate degradation
ko00630	1.03	1.05	Glyoxylate and dicarboxylate metabolism
ko00633	0.87	0.77	Nitrotoluene degradation
ko00642	0.01	0.02	Ethylbenzene degradation
ko00643	0.01	0.03	Styrene degradation
ko00791	0.00	0.02	Atrazine degradation
ko00903	0.27	0.29	Limonene and pinene degradation
ko00930	0.18	0.20	Caprolactam degradation
Total	3.97	4.31	

4.3. Influence of Key Microbes on SGD in Qinzhou Bay

Generally, submarine groundwater systems contaminated by organic matter are electron-acceptor limited and are in reducing environments [9,73]. As a result of DOC oxidation, SGD may be depleted in NO_3^- and enriched in reduced metabolites such as dissolved Fe(II) [74,75]. Furthermore, aquifer systems often contain solid phase organic matter with minerals such as pyrite, siderite and Fe(II) silicates, which can reduce suitable oxidants such as NO_3^- or oxygen [76–78]. Excess SGD-derived nutrients, carbon and metals have been recognized to have deleterious effects on marine ecological environments. Microorganisms are recognized as important participants in biogeochemical processes in the SGD [22]. In Figure 7, Fe(II)-oxidizing and nitrate-reducing processes occur in FeOB in the >0.45 μm size fraction, and then generate Fe(III) mineral precipitation and N_2, respectively [37,79]. These processes could reduce nitrate in SGD. Both *Bathyarchaeota* in the >0.45 μm size fraction and *Novosphingobium* spp. in the >0.45 μm size fraction and 0.2–0.45 μm fraction could degrade aromatic compounds [55,65]. The *Methanosaeta* and *Limnohabitans* spp. could consume acetate produced by *Bathyarchaeota* fermentation and then generate CH_4 and CO_2, respectively ([36,56,57]. Meanwhile, the *Limnohabitans* spp. could utilize the DOM as an important source of substrates [70–72]. Submarine groundwater often contains higher concentrations of nutrients, carbon, and metals than river water and seawater [3,9]. However, the concentrations of NO_3^- (5.2 μmol L^{-1}) and DOC (1.0 mmol L^{-1}) in our studied submarine groundwater were lower than those (NO_3^-: 7.2 μmol L^{-1}; DOC: 1.1 mmol L^{-1}) in the seawater of Qinzhou Bay. We suggest that the lower NO_3^- and DOC concentrations in our studied submarine groundwater are the result of the metabolic action of these bacteria and the archaea. In addition, the concentrations of DIN and DOC in global submarine groundwater were 211 μmol L^{-1} and 1.8 mmol L^{-1} [12,80], which significantly higher than those (DIN: 10.4 μmol L^{-1}; DOC: 1.0 mmol L^{-1}) in the submarine groundwater of Qinzhou Bay. This further indicates that nutrients and the carbon of submarine groundwater may be utilized by these microorganisms in our study site. In view of this, the dominant microbes of the two size fractions in the studied submarine groundwater of Qinzhou Bay were likely involved in the degradation or consumption of organic pollutants and excess nutrients, such as aromatic compounds, nitrates and DOM. These dominant microbes will be expected to reduce the amount of organic pollutants and excess nutrients from SGD entering coastal water, which may impact carbon, nitrogen and iron cycling in SGD (Figure 7).
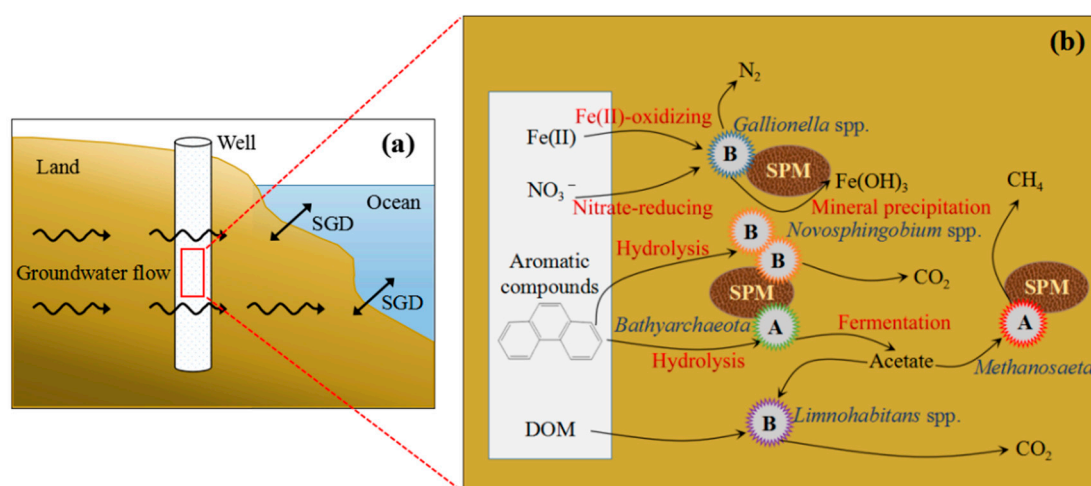

Figure 7. Schematic diagram of submarine groundwater discharge (SGD) (**a**). Main mechanism of nitrate, carbon and iron depletion contributed by the dominant microbial community of SGD in Qinzhou Bay (**b**). The "Suspended particulate matter (SPM)" in ovals represents suspended particulate matter. The "A" and "B" in the star with different colors represent the specific archaeal and bacterial groups, respectively.

5. Conclusions

In this study, we investigated the microbial assemblages from two size fractions in submarine groundwater near an industrial zone, Qinzhou Bay. The main bacterial and archaeal groups in the >0.45 μm size fraction and 0.2–0.45 μm fraction communities were significantly different, based on a PERMANOVA test. Moreover, some potential key microbial groups from two size fractions were also involved in the utilization and conversion of biogenic elements such as carbon, nutrients and iron. For example, *Bathyarchaeota* was detected in the >0.45 μm size fraction and *Novosphingobium* spp. were found in both the >0.45 μm size fraction and the 0.2–0.45 μm fraction, indicating that these genera play an important role in the degradation of aromatic compounds. *Gallionella* spp. were most abundant in the >0.45 μm size fraction and could consume nitrate and produce N_2 while oxidizing Fe(II) to Fe(III) mineral precipitation, reflecting that this genus could consume a part of the nitrate in SGD before flowing into coastal water. These results showed that microbial communities may have potential roles in carbon, nitrogen and iron cycling in submarine groundwater systems (subterranean estuary).

In addition, the dominant bacterial sequences in the 0.2–0.45 μm fraction were affiliated with *Limnohabitans* spp., which could utilize DOM as an important source of substrates. Therefore, the *Bathyarchaeota*, *Novosphingobium* spp., *Limnohabitans* spp. and *Gallionella* spp. could be selected as microbial candidates for in situ biodegradation or bioremediation in the polluted subterranean estuary by aromatic compounds, excess nitrates and DOM. Both functional metagenomic analyses of the structure, function and culture experiments of isolating specific microbes for in situ bioremediation in the subterranean estuary, such as the aquifer along the coast of Qinzhou Bay (i.e., the polluted coastal zone by a petroleum refinery), are necessary to further any research in the future.

References

1. Burnett, W.C.; Bokuniewicz, H.; Huettel, M.; Moore, W.S.; Taniguchi, M. Groundwater and pore water inputs to the coastal zone. *Biogeochemistry* **2003**, *66*, 3–33. [CrossRef]
2. Moore, W.S. The subterranean estuary: A reaction zone of ground water and sea water. *Mar. Chem.* **1999**, *65*, 111–125. [CrossRef]
3. Moore, W.S. The effect of submarine groundwater discharge on the ocean. *Annu. Rev. Mar. Sci.* **2010**, *2*, 59–88. [CrossRef] [PubMed]
4. Pavlidou, A.; Papadopoulos, V.P.; Hatzianestis, I.; Simboura, N.; Patiris, D.; Tsabaris, C. Chemical inputs from a karstic submarine groundwater discharge (SGD) into an oligotrophic Mediterranean coastal area. *Sci. Total Environ.* **2014**, *488*, 1–13. [CrossRef] [PubMed]
5. Chen, X.; Wang, J.; Cukrov, N.; Du, J. Porewater-derived nutrient fluxes in a coastal aquifer (Shengsi Island, China) and its implication. *Estuar. Coast. Shelf Sci.* **2019**, *218*, 204–211. [CrossRef]
6. Luo, X.; Jiao, J.J. Submarine groundwater discharge and nutrient loadings in Tolo Harbor, Hong Kong using multiple geotracer-based models, and their implications of red tide outbreaks. *Water Res.* **2016**, *102*, 11–31. [CrossRef] [PubMed]
7. Hwang, D.; Lee, Y.W.; Kim, G. Large submarine groundwater discharge and benthic eutrophication in Bangdu Bay on volcanic Jeju Island, Korea. *Limnol. Oceanogr.* **2005**, *50*, 1393–1403. [CrossRef]

8.   McCoy, C.; Viso, R.; Peterson, R.N.; Libes, S.; Lewis, B.; Ledoux, J.; Voulgaris, G.; Smith, E.; Sanger, D. Radon as an indicator of limited cross-shelf mixing of submarine groundwater discharge along an open ocean beach in the South Atlantic Bight during observed hypoxia. *Cont. Shelf Res.* **2011**, *31*, 1306–1317. [CrossRef]

9.   Slomp, C.P.; Van Cappellen, P. Nutrient inputs to the coastal ocean through submarine groundwater discharge: Controls and potential impact. *J. Hydrol.* **2004**, *295*, 64–86. [CrossRef]

10.   UNESCO. *Submarine Groundwater Discharge: Management Implications, Measurements and Effects*; IHP-VI, Series on Groundwater No. 5, IOC Manuals and Guides No. 44; UNESCO: Paris, France, 2004.

11.   Chen, X.; Lao, Y.; Wang, J.; Du, J.; Liang, M.; Yang, B. Submarine Groundwater-Borne Nutrients in a Tropical Bay (Maowei Sea, China) and Their Impacts on the Oyster Aquaculture. *Geochem. Geophys. Geosyst.* **2018**, *19*, 932–951. [CrossRef]

12.   Chen, X.; Zhang, F.; Lao, Y.; Wang, X.; Du, J.; Santos, I.R. Submarine groundwater discharge-derived carbon fluxes in mangroves: An important component of blue carbon budgets? *J. Geophys. Res. Oceans* **2018**, *123*, 6962–6979. [CrossRef]

13.   Zhang, J.L.; Li, Y.Y.; Wang, Y.H.; Zhang, Y.Y.; Zhang, D.; Zhang, R.J.; Li, Y.; Zhang, G. Spatial distribution and ecological risk of polychlorinated biphenyls in sediments from Qinzhou Bay, Beibu Gulf of South China. *Mar. Pollut. Bull.* **2014**, *80*, 338–343. [CrossRef] [PubMed]

14.   Gu, Y.G.; Lin, Q.; Yu, Z.L.; Wang, X.N.; Ke, C.L.; Ning, J.J. Speciation and risk of heavy metals in sediments and human health implications of heavy metals in edible nekton in Beibu Gulf, China: A case study of Qinzhou Bay. *Mar. Pollut. Bull.* **2015**, *101*, 852–859. [CrossRef] [PubMed]

15.   Turner, A.; Millward, G.E. Suspended particles: Their role in estuarine biogeochemical cycles. *Estuar. Coast. Shelf Sci.* **2002**, *55*, 857–883. [CrossRef]

16.   Suzumura, M.; Kokubun, H.; Arata, N. Distribution and characteristics of suspended particulate matter in a heavily eutrophic estuary, Tokyo Bay, Japan. *Mar. Pollut. Bull.* **2004**, *49*, 496–503. [CrossRef] [PubMed]

17.   Rosa, F.; Bloesch, J.; Rathke, D.E. Sampling the settling and suspended particulate matter (SPM). In *Handbook of Techniques for Aquatic Sediments Sampling*; Murdoch, A., MacKnight, S.D., Eds.; CRC Press: Boca Raton, FL, USA, 1994; pp. 97–129.

18.   Uncles, R.J.; Joint, I.; Stephens, J.A. Transport and retention of suspended particulate matter and bacteria in the Humber-Ouse Estuary, United Kingdom, and their relationship to hypoxia and anoxia. *Estuaries* **1998**, *21*, 597–612. [CrossRef]

19.   Kravchishina, M.D.; Mitzkevich, I.N.; Veslopolova, E.F.; Shevchenko, V.P.; Lisitzin, A.P. Relationship between the suspended particulate matter and microorganisms in the White Sea waters. *Oceanology* **2008**, *48*, 837–854. [CrossRef]

20.   Perkins, T.L.; Perrow, K.; Rajko-Nenow, P.; Jago, C.F.; Jones, D.L.; Malham, S.K.; McDonald, J.E. Decay rates of faecal indicator bacteria from sewage and ovine faeces in brackish and freshwater microcosms with contrasting suspended particulate matter concentrations. *Sci. Total Environ.* **2016**, *572*, 1645–1652. [CrossRef]

21.   Boehm, A.B.; Shellenbarger, G.G.; Paytan, A. Groundwater discharge: Potential association with fecal indicator bacteria in the surf zone. *Environ. Sci. Technol.* **2004**, *38*, 3558–3566. [CrossRef]

22.   Ye, Q.; Liu, J.A.; Du, J.Z.; Zhang, J. Bacterial diversity in submarine groundwater along the coasts of the yellow sea. *Front. Microbiol.* **2016**, *6*, 1519. [CrossRef]

23.   Halliday, E.; Gast, R.J. Bacteria in beach sands: An emerging challenge in protecting coastal water quality and bather health. *Environ. Sci. Technol.* **2010**, *45*, 370–379. [CrossRef] [PubMed]

24.   Liu, S.M.; Hong, G.H.; Zhang, J.; Ye, X.W.; Jiang, X.L. Nutrient budgets for large Chinese estuaries. *Biogeosciences* **2009**, *6*, 2245–2263. [CrossRef]

25.   Cerdà-Domènech, M.; Rodellas, V.; Folch, A.; Garcia-Orellana, J. Constraining the temporal variations of Ra isotopes and Rn in the groundwater end-member: Implications for derived SGD estimates. *Sci. Total Environ.* **2017**, *595*, 849–857. [CrossRef] [PubMed]

26.   Xiong, J.; Liu, Y.; Lin, X.; Zhang, H.; Zeng, J.; Hou, J.; Yang, Y.; Yao, T.; Knight, R.; Chu, H. Geographic distance and pH drive bacterial distribution in alkaline lake sediments across Tibetan Plateau. *Environ. Microbiol.* **2012**, *14*, 2457–2466. [CrossRef] [PubMed]

27.   Pires, A.C.C.; Cleary, D.F.R.; Almeida, A.; Cunha, A.; Dealtry, S.; Mendonça-Hagler, L.C.S.; Smalla, K.; Gomes, N.C. Denaturing gradient gel electrophoresis and barcoded pyrosequencing reveal unprecedented archaeal diversity in mangrove sediment and rhizosphere samples. *Appl. Environ. Microbiol.* **2012**, *78*, 5520–5528. [CrossRef] [PubMed]

28. Caporaso, J.G.; Kuczynski, J.; Stombaugh, J.; Bittinger, K.; Bushman, F.D.; Costello, E.K.; Fierer, N.; Peña, A.G.; Goodrich, J.K.; Gordon, J.I.; et al. QIIME allows analysis of high throughput community sequencing data. *Nat. Methods* **2010**, *7*, 335–336. [CrossRef]

29. Li, Y.F.; Chen, Y.R.; Yang, J.L.; Bao, W.Y.; Guo, X.; Liang, X.; Shi, Z.Y.; Li, J.-L.; Ding, D.-W. Effects of substratum type on bacterial community structure in biofilms in relation to settlement of plantigrades of the mussel *Mytilus coruscus*. *Int. Biodeter. Biodegr.* **2014**, *96*, 41–49. [CrossRef]

30. Tamura, K.; Stecher, G.; Peterson, D.; Filipski, A.; Kumar, S. MEGA6: Molecular evolutionary genetics analysis version 6.0. *Mol. Biol. Evol.* **2013**, *30*, 2725–2729. [CrossRef]

31. Schloss, P.D.; Westcott, S.L.; Ryabin, T.; Hall, J.R.; Hartmann, M.; Hollister, E.B.; Lesniewski, R.A.; Oakley, B.B.; Parks, D.H.; Robinson, C.J.; et al. Introducing mothur: Open-source, platform-independent, community-supported software for describing and comparing microbial communities. *Appl. Environ. Microbiol.* **2009**, *75*, 7537–7541. [CrossRef]

32. Langille, M.G.; Zaneveld, J.; Caporaso, J.G.; McDonald, D.; Knights, D.; Reyes, J.A.; Clemente, J.C.; Burkepile, D.R.; Thurber, R.V.; Knight, R.; et al. Predictive functional profiling of microbial communities using 16S rRNA marker gene sequences. *Nat. Biotechnol.* **2013**, *31*, 814. [CrossRef]

33. Cho, H.M.; Kim, G. Determining groundwater Ra end-member values for the estimation of the magnitude of submarine groundwater discharge using Ra isotope tracers. *Geophys. Res. Lett.* **2016**, *43*, 3865–3871. [CrossRef]

34. Fabisch, M.; Beulig, F.; Akob, D.M.; Küsel, K. Surprising abundance of Gallionella-related iron oxidizers in creek sediments at pH 4.4 or at high heavy metal concentrations. *Front. Microbiol.* **2013**, *4*, 390. [CrossRef] [PubMed]

35. Hahn, M.W.; Kasalický, V.; Jezbera, J.; Brandt, U.; Šimek, K. *Limnohabitans australis* sp. nov., isolated from a freshwater pond, and emended description of the genus *Limnohabitans*. *Int. J. Syst. Evol. Microbiol.* **2010**, *60*, 2946–2950. [CrossRef] [PubMed]

36. Kasalický, V.; Jezbera, J.; Šimek, K.; Hahn, M.W. *Limnohabitans planktonicus* sp. nov. and *Limnohabitans parvus* sp. nov., planktonic betaproteobacteria isolated from a freshwater reservoir, and emended description of the genus *Limnohabitans*. *Int. J. Syst. Evol. Microbiol.* **2010**, *60*, 2710–2714. [CrossRef]

37. Blöthe, M.; Roden, E.E. Composition and activity of an autotrophic Fe (II)-oxidizing, nitrate-reducing enrichment culture. *Appl. Environ. Microbiol.* **2009**, *75*, 6937–6940. [CrossRef] [PubMed]

38. Klein, A.N.; Frigon, D.; Raskin, L. Populations related to *Alkanindiges*, a novel genus containing obligate alkane degraders, are implicated in biological foaming in activated sludge systems. *Environ. Microbiol.* **2007**, *9*, 1898–1912. [CrossRef]

39. Sohn, J.H.; Kwon, K.K.; Kang, J.H.; Jung, H.B.; Kim, S.J. *Novosphingobium pentaromativorans* sp. nov., a high-molecular-mass polycyclic aromatic hydrocarbon-degrading bacterium isolated from estuarine sediment. *Int. J. Syst. Evol. Microbiol.* **2004**, *54*, 1483–1487. [CrossRef]

40. Choi, J.H.; Kim, M.S.; Jung, M.J.; Roh, S.W.; Shin, K.S.; Bae, J.W. *Sphingopyxis soli* sp. nov., isolated from landfill soil. *Int. J. Syst. Evol. Microbiol.* **2010**, *60*, 1682–1686. [CrossRef]

41. Lee, S.; Weon, H.Y.; Kim, S.J.; Ahn, T.Y. *Flavobacterium koreense* sp. nov., *Flavobacterium chungnamense* sp. nov., and *Flavobacterium cheonanense* sp. nov., isolated from a freshwater reservoir. *J. Microbiol.* **2011**, *49*, 387–392. [CrossRef]

42. LaFrentz, B.R.; Waldbieser, G.C.; Welch, T.J.; Shoemaker, C.A. Intragenomic heterogeneity in the 16S rRNA genes of *Flavobacterium columnare* and standard protocol for genomovar assignment. *J. Fish Dis.* **2014**, *37*, 657–669. [CrossRef]

43. Enright, A.M.; McGrath, V.; Gill, D.; Collins, G.; O'Flaherty, V. Effect of seed sludge and operation conditions on performance and archaeal community structure of low-temperature anaerobic solvent-degrading bioreactors. *Syst. Appl. Microbiol.* **2009**, *32*, 65–79. [CrossRef] [PubMed]

44. Kasai, Y.; Takahata, Y.; Hoaki, T.; Watanabe, K. Physiological and molecular characterization of a microbial community established in unsaturated, petroleum-contaminated soil. *Environ. Microbiol.* **2005**, *7*, 806–818. [CrossRef] [PubMed]

45. Barber, R.D.; Zhang, L.; Harnack, M.; Olson, M.V.; Kaul, R.; Ingram-Smith, C.; Smith, K.S. Complete genome sequence of *Methanosaeta concilii*, a specialist in aceticlastic methanogenesis. *J. Bacteriol.* **2011**, *193*, 3668–3669. [CrossRef] [PubMed]

46. Llirós, M.; Casamayor, E.O.; Borrego, C. High archaeal richness in the water column of a freshwater sulfurous karstic lake along an interannual study. *FEMS Microbiol. Ecol.* **2008**, *66*, 331–342. [CrossRef] [PubMed]

47. Conrad, R.; Klose, M.; Noll, M.; Kemnitz, D.; Bodelier, P.L. Soil type links microbial colonization of rice roots to methane emission. *Glob. Chang. Biol.* **2008**, *14*, 657–669. [CrossRef]

48. Castelle, C.J.; Wrighton, K.C.; Thomas, B.C.; Hug, L.A.; Brown, C.T.; Wilkins, M.J.; Frischkorn, K.R.; Tringe, S.G.; Singh, A.; Markillie, L.M.; et al. Genomic expansion of domain archaea highlights roles for organisms from new phyla in anaerobic carbon cycling. *Curr. Biol.* **2015**, *25*, 690–701. [CrossRef]

49. Kubo, K.; Lloyd, K.G.; Biddle, J.F.; Amann, R.; Teske, A.; Knittel, K. Archaea of the Miscellaneous Crenarchaeotal Group are abundant, diverse and widespread in marine sediments. *ISME J.* **2012**, *6*, 1949–1965. [CrossRef]

50. Lloyd, K.G.; Schreiber, L.; Petersen, D.G.; Kjeldsen, K.U.; Lever, M.A.; Steen, A.D.; Stepanauskas, R.; Richter, M.; Kleindienst, S.; Lenk, S.; et al. Predominant archaea in marine sediments degrade detrital proteins. *Nature* **2013**, *496*, 215–218. [CrossRef]

51. Evans, P.N.; Parks, D.H.; Chadwick, G.L.; Robbins, S.J.; Orphan, V.J.; Golding, S.D.; Tyson, G.W. Methane metabolism in the archaeal phylum Bathyarchaeota revealed by genome-centric metagenomics. *Science* **2015**, *350*, 434–438. [CrossRef]

52. Lazar, C.S.; Baker, B.J.; Seitz, K.; Hyde, A.S.; Dick, G.J.; Hinrichs, K.U.; Teske, A.P. Genomic evidence for distinct carbon substrate preferences and ecological niches of *Bathyarchaeota* in estuarine sediments. *Environ. Microbiol.* **2016**, *18*, 1200–1211. [CrossRef]

53. Fry, J.C.; Parkes, R.J.; Cragg, B.A.; Weightman, A.J.; Webster, G. Prokaryotic biodiversity and activity in the deep subseafloor biosphere. *FEMS Microbiol. Ecol.* **2008**, *66*, 181–196. [CrossRef] [PubMed]

54. Meng, J.; Xu, J.; Qin, D.; He, Y.; Xiao, X.; Wang, F. Genetic and functional properties of uncultivated MCG archaea assessed by metagenome and gene expression analyses. *ISME J.* **2014**, *8*, 650–659. [CrossRef] [PubMed]

55. He, Y.; Li, M.; Perumal, V.; Feng, X.; Fang, J.; Xie, J.; Sievert, S.M.; Wang, F. Genomic and enzymatic evidence for acetogenesis among multiple lineages of the archaeal phylum *Bathyarchaeota* widespread in marine sediments. *Nat. Microbiol.* **2016**, *1*, 16035. [CrossRef] [PubMed]

56. Xiang, X.; Wang, R.; Wang, H.; Gong, L.; Man, B.; Xu, Y. Distribution of Bathyarchaeota Communities Across Different Terrestrial Settings and Their Potential Ecological Functions. *Sci. Rep.* **2017**, *7*, 45028. [CrossRef] [PubMed]

57. Ma, K.; Liu, X.; Dong, X. *Methanosaeta harundinacea* sp. nov., a novel acetate-scavenging methanogen isolated from a UASB reactor. *Int. J. Syst. Evol. Microbiol.* **2006**, *56*, 127–131. [CrossRef] [PubMed]

58. Guo, W.; He, M.; Yang, Z.; Lin, C.; Quan, X.; Wang, H. Distribution of polycyclic aromatic hydrocarbons in water, suspended particulate matter and sediment from Daliao River watershed, China. *Chemosphere* **2007**, *68*, 93–104. [CrossRef] [PubMed]

59. Hwang, C.; Wu, W.; Gentry, T.J.; Carley, J.; Corbin, G.A.; Carroll, S.L.; Watson, D.B.; Jardine, P.M.; Zhou, J.; Criddle, C.S.; et al. Bacterial community succession during in situ uranium bioremediation: Spatial similarities along controlled flow paths. *ISME J.* **2009**, *3*, 47–64. [CrossRef]

60. Gan, H.M.; Hudson, A.O.; Rahman, A.Y.A.; Chan, K.G.; Savka, M.A. Comparative genomic analysis of six bacteria belonging to the genus *Novosphingobium*: Insights into marine adaptation, cell-cell signaling and bioremediation. *BMC Genom.* **2013**, *14*, 431. [CrossRef]

61. Yabuuchi, E.; Yano, I.; Oyaizu, H.; Hashimoto, Y.; Ezaki, T.; Yamamoto, H. Proposals of *Sphingomonas paucimobilis* gen. nov. and comb. nov., *Sphingomonas parapaucimobilis* sp. nov., *Sphingomonas yanoikuyae* sp. nov., *Sphingomonas adhaesiva* sp. nov., *Sphingomonas capsulata* comb. nov., and two genospecies of the genus Sphingomonas. *Microbiol. Immunol.* **1990**, *34*, 99–119. [CrossRef]

62. Tiirola, M.A.; Männistö, M.K.; Puhakka, J.A.; Kulomaa, M.S. Isolation and characterization of *Novosphingobium* sp. strain MT1, a dominant polychlorophenol-degrading strain in a groundwater bioremediation system. *Appl. Environ. Microbiol.* **2002**, *68*, 173–180. [CrossRef]

63. Yan, Q.X.; Hong, Q.; Han, P.; Dong, X.J.; Shen, Y.J.; Li, S.P. Isolation and characterization of a carbofuran-degrading strain *Novosphingobium* sp. FND-3. *FEMS Microbiol. Lett.* **2007**, *271*, 207–213. [CrossRef] [PubMed]

64. Yuan, J.; Lai, Q.; Zheng, T.; Shao, Z. *Novosphingobium indicum* sp. nov., a polycyclic aromatic hydrocarbon-degrading bacterium isolated from a deep-sea environment. *Int. J. Syst. Evol. Microbiol.* **2009**, *59*, 2084–2088. [CrossRef] [PubMed]

65. Hashimoto, T.; Onda, K.; Morita, T.; Luxmy, B.S.; Tada, K.; Miya, A.; Murakami, T. Contribution of the estrogen-degrading bacterium *Novosphingobium* sp. strain JEM-1 to estrogen removal in wastewater treatment. *J. Environ. Eng.* **2010**, *136*, 890–896. [CrossRef]

66. Kappler, A.; Straub, K.L. Geomicrobiological cycling of iron. *Rev. Mineral. Geochem.* **2005**, *59*, 85–108. [CrossRef]

67. Konhauser, K.O.; Amskold, L.; Lalonde, S.V.; Posth, N.R.; Kappler, A.; Anbar, A. Decoupling photochemical Fe (II) oxidation from shallow-water BIF deposition. *Earth Planet. Sci. Lett.* **2007**, *258*, 87–100. [CrossRef]

68. Pérez, M.T.; Sommaruga, R. Differential effect of algal-and soil-derived dissolved organic matter on alpine lake bacterial community composition and activity. *Limnol. Oceanogr.* **2006**, *51*, 2527–2537. [CrossRef]

69. Šimek, K.; Kasalický, V.; Zapomělová, E.; Horňák, K. Alga-derived substrates select for distinct betaproteobacterial lineages and contribute to niche separation in *Limnohabitans* strains. *Appl. Environ. Microbiol.* **2011**, *77*, 7307–7315. [CrossRef]

70. Hörtnagl, P.; Pérez, M.T.; Zeder, M.; Sommaruga, R. The bacterial community composition of the surface microlayer in a high mountain lake. *FEMS Microbiol. Ecol.* **2010**, *73*, 458–467. [CrossRef]

71. Glaeser, S.P.; Grossart, H.P.; Glaeser, J. Singlet oxygen, a neglected but important environmental factor: Short-term and long-term effects on bacterioplankton composition in a humic lake. *Environ. Microbiol.* **2010**, *12*, 3124–3136. [CrossRef]

72. Kasalický, V.; Jezbera, J.; Hahn, M.W.; Šimek, K. The diversity of the *Limnohabitans genus*, an important group of freshwater bacterioplankton, by characterization of 35 isolated strains. *PLoS ONE* **2013**, *8*, e58209. [CrossRef]

73. Chapelle, F. *Ground-Water Microbiology and Geochemistry*; John Wiley & Sons: New York, NY, USA, 2001.

74. Chapelle, F.H.; Lovley, D.R. Competitive exclusion of sulfate reduction by Fe (III)-reducing bacteria: A mechanism for producing discrete zones of high-iron ground water. *Groundwater* **1992**, *30*, 29–36. [CrossRef]

75. Appelo, C.A.J.; Postma, D. *Geochemistry, Groundwater and Pollution*; Balkema: Amsterdam, The Netherlands, 1994.

76. Postma, D.; Boesen, C.; Kristiansen, H.; Larsen, F. Nitrate reduction in an unconfined sandy aquifer: Water chemistry, reduction processes, and geochemical modeling. *Water Resour. Res.* **1991**, *27*, 2027–2045. [CrossRef]

77. Engesgaard, P.; Kipp, K.L. A geochemical transport model for redox-controlled movement of mineral fronts in groundwater flow systems: A case of nitrate removal by oxidation of pyrite. *Water Resour. Res.* **1992**, *28*, 2829–2843. [CrossRef]

78. Hartog, N.; Griffioen, J.; van der Weijden, C.H. Distribution and reactivity of O_2-reducing components in sediments from a layered aquifer. *Environ. Sci. Technol.* **2002**, *36*, 2338–2344. [CrossRef] [PubMed]

79. Straub, K.L.; Benz, M.; Schink, B.; Widdel, F. Anaerobic, nitrate-dependent microbial oxidation of ferrous iron. *Appl. Environ. Microbiol.* **1996**, *62*, 1458–1460. [PubMed]

80. Cho, H.M.; Kim, G.; Kwon, E.Y.; Moosdorf, N.; Garcia-Orellana, J.; Santos, I.R. Radium tracing nutrient inputs through submarine groundwater discharge in the global ocean. *Sci. Rep.* **2018**, *8*, 2439. [CrossRef] [PubMed]